Inorganic Chemistry

pubs.acs.org/IC

Communication

Metal/Support Interactions Regulate Substrate Binding in Fe/Co/Se Cluster Catalysts

Benjamin S. Mitchell, Andrei Chirila, Daniel Y. Zhou, Jonathan A. Kephart, and Alexandra Velian*

Cite This: *Inorg. Chem.* 2023, 62, 8789−8793

Read Online

ACCESS | Metrics & More | Article Recommendations | Supporting Information

ABSTRACT: Here, we investigate the stereoelectronic requirements of a family of Fe/Co_6Se_8 molecular clusters to achieve a Goldilocks regime of substrate affinity for the catalytic coupling of tosyl azide and *tert*-butyl isocyanide. The reactivity of a catalytically competent iron-nitrenoid intermediate, observed *in situ*, is explored toward nitrene transfer and hydrogen-atom abstraction. The dual role of isocyanide, which, on the one hand, prevents catalyst degradation but, in large amounts, slows down reactivity, is exposed. The impact of distal changes (the number of neighboring active sites and the identity of supporting ligands) on the substrate affinity, electronic properties, and catalytic activity is investigated. Overall, the study reveals that the dynamic, push−pull interactions between the substrate (^{t}BuNC), active site (Fe), and support (Co_6Se_8) create a regime where increased substrate activation occurs with facile dissociation.

The Sabatier principle intuitively states that optimal catalytic activity is reached when the active site has a moderate affinity for substrates or the resulting products, underscoring the tension between engaging and releasing key adsorbates that ensures continuous reactivity at the active sites.[1−3] While weak adsorption may limit reactions from occurring, strong substrate/active site interactions can inhibit catalytic turnovers by blocking the active site or by electronically deactivating neighboring ones.[4] Structurally uniform platforms enable systematic studies that uncover the requirements for optimal conditions of adsorbate/active site interactions for a given transformation and elucidate the nature of the cooperativity between the active site and the support. For example, numerous *in silico* and experimental studies have shown how the size, morphology, dopants, or active site identity in the single-layer limit of MoS_2 clusters impacts the strength of adsorbate/catalyst interactions[5−9] and breaks linear scaling relationships.[10]

Elucidating how multiple metals cooperate to bind and activate substrates to unearth catalyst design principles for complex multielectron transformations is the focus of numerous molecular efforts.[11−14] To this end, our group introduced a molecular construct in which the identity and number of active sites installed on an atomically precise inorganic cluster support can be systematically tuned.[15−19] This synthetic innovation has enabled systematic investigations into the nature of the active site/support cooperativity[15,16] and the role of multiactive site dynamics in modulating the catalytic activity for azide activation and asymmetric carbodiimide synthesis.[18]

In this study, we investigate the stereoelectronic requirements of the active site to access a Goldilocks regime of substrate affinity in a family of Fe/Co_6Se_8 molecular cluster catalysts (Figure 1).[20] Distal changes, such as the number of neighboring active sites and the identity of supporting ligands, impact the substrate affinity and modulate the ensuing catalytic activity toward coupling tosyl azide and *tert*-butyl isocyanide. The study uncovers how the dynamic substrate/active site/support interactions coalesce to maximize the catalytic activity. Strong metal/support interactions promote substrate (isocyanide) dissociation, while simultaneously enabling π-back-bonding and increased substrate activation. Additionally, this study illustrates the duality of isocyanide as a substrate: on the one hand, the isocyanide prevents catalyst degradation, but, in large amounts, it slows down reactivity ostensibly by blocking the active site. The nature of the metal−support interactions, the presence of multiple substrate binding sites, and the steric profile at the active site dramatically alter the observed catalytic activity toward nitrene transfer and carbodiimide formation.[17]

We have previously isolated catalytically competent metal imido intermediates at a trichromium cluster, demonstrating that the edges are the locus of reactivity.[18] In contrast, the identification of iron nitrenoid intermediates for the triiron $Fe_3Co_6Se_8L_6$ (**2**-Fe_3; L = $PPh_2N^{(-)}$Tol, Ph = phenyl, and Tol = 4-tolyl) or monoiron derivative $FeCo_6Se_8(PEt_3)_4(L)_2$ (**1**-Fe; Et = ethyl) has been elusive.[15,16] We hypothesized that the presence of a single active site could make observing intermediates and interpreting the reactivity of **1**-Fe more accessible than those for the triiron congener **2**-Fe_3. Indeed, at 10% **1**-Fe loading, we have previously observed the formation of two paramagnetic species by ^{1}H NMR spectroscopy during the course of carbodiimide formation.[15] To probe the identity of these species, here, the reaction between **1**-Fe and TsN_3 was evaluated first under stoichiometric conditions (Scheme 1).

Received: May 16, 2023
Published: May 25, 2023

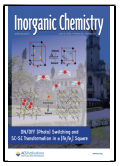

https://doi.org/10.1021/acs.inorgchem.3c01601
Inorg. Chem. 2023, 62, 8789−8793

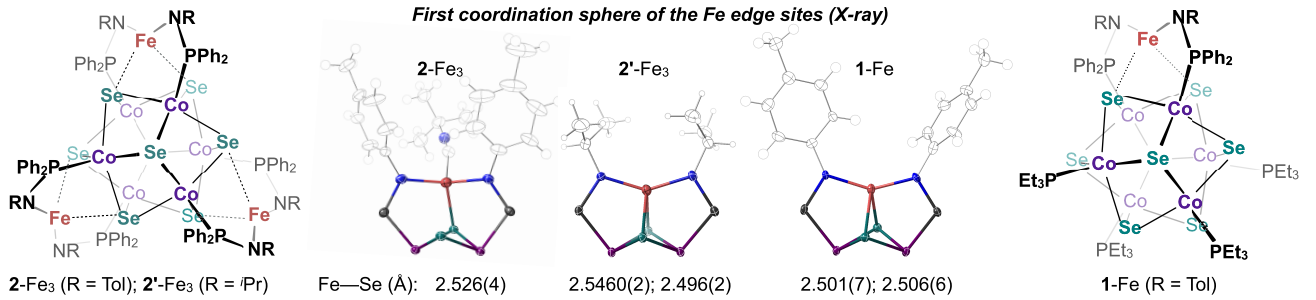

Figure 1. Connectivity and first coordination sphere of the Fe-edge sites in **2**-Fe_3, **2′**-Fe_3, and **1**-Fe from previously reported single-crystal X-ray structures.[15,16,28]

Slow addition of the azide to a thawing solution of the iron complex leads to rapid effervescence and consumption of the azide, as is evinced by the disappearance of the diagnostic tosyl azide stretch (2123 cm^{-1}; Figure S2) in the associated IR spectrum. Analysis of the crude reaction mixture by ^{1}H and ^{31}P NMR spectroscopy indicates the complete conversion of **1**-Fe to two new species assigned as **1**-Fe(NTs) and **1**-Fe(NHTs) and formed in a 4:1 molar ratio (Scheme 1 and Figures S1 and S3). The ability of only one of the species to transfer the nitrene group and regenerate **1**-Fe led to its identification as **1**-Fe(NTs). Indeed, treating a freshly prepared mixture of these two species with stoichiometric isocyanide[21] (^{t}BuNC) incurs the complete consumption of **1**-Fe(NTs), while **1**-Fe(NHTs) remains unreacted (Figure S7). The starting material **1**-Fe is regenerated quantitatively, along with the corresponding nitrene transfer product. Similar results are obtained if a phosphine[22] ($PPhMe_2$) is used instead to trap the nitrene group, giving rise to the iminophosphorane coproduct $TsNPPhMe_2$ (Figures S4 and S5).

Iron nitrenoid complexes are often difficult to isolate due to their reactive iminyl character favoring hydrogen abstraction chemistry.[23,24] To probe the identity of the azide activation coproduct, ostensibly **1**-Fe(NHTs), a well-known hydrogen-atom source, 9,10-dihydroanthracene (DHA; 15 or 30 equiv),[25] was added to the reaction between **1**-Fe and TsN_3 (Scheme 2a and Section S2.4). After 4 h at 60 °C, ^{1}H NMR spectroscopy indicates that no **1**-Fe(NTs) persists in the reaction mixture. Instead, the dominant species is the amido complex **1**-Fe(NHTs), generated alongside intractable paramagnetic byproducts (Figures S8−S10). The relatively slow reaction between **1**-Fe(NTs) and DHA, perhaps due to the steric bulk at Fe, fosters decomposition. Increasing the DHA amount from 15 to 30 equiv enhances the conversion to **1**-Fe(NHTs) from ca. 54 to 70% spectroscopic yield (Figure S11). Similar results are obtained using other hydrogen-atom donors (Section S2.5).[25−27] Over time or upon purification attempts, both **1**-Fe(NTs) and **1**-Fe(NHTs) degrade, precluding their separation or further characterization as pure species.

Increased isocyanide concentration could accelerate nitrene transfer and prevent hydrogen abstraction chemistry. Indeed, at 10% **1**-Fe loading and a large excess of isocyanide (500 equiv; 5.6 M), the formation of **1**-Fe(NHTs) is entirely prevented (Scheme 2b and Figure S16). In contrast, at low isocyanide concentration (19 equiv, 0.2 M), ca. 40% of the cluster is consumed in the off-cycle formation of **1**-Fe(NHTs).[15] The triiron cluster **2**-Fe_3 shows a similar stability profile,[16] its decomposition is shut off in the presence of a large excess of a coordinating ligand (*tert*-butyl isocyanide or pyridine; Figures S15 and S17).[16]

To uncover how the number of edge sites and the isocyanide concentration modulate the catalytic activity, **1**-Fe and **2**-Fe_3 are compared under high isocyanide concentration, when both clusters are recovered quantitatively. **2**-Fe_3 features 3 times more Fe-edge sites than **1**-Fe, yet under the same conditions (2.5% cluster loading, 5.6 M ^{t}BuNC), **1**-Fe reaches 50% conversion ($t_{1/2}$) significantly faster than **2**-Fe_3 (ca. 10 vs 50 min; Figure 2). This indicates that, although the edge sites in **1**-Fe and **2**-Fe_3 have chemically identical first coordination environments, the former is significantly more reactive. We hypothesized that the difference in reactivity between **1**-Fe and **2**-Fe_3 is a result of modulating the electronic richness of the active site by distal changes in the cluster (the number of active sites or ancillary ligands), which, in turn, regulates the affinity for substrates (^{t}BuNC). To probe this hypothesis, $Fe_3Co_6Se_8L'_6$ (**2′**-Fe_3 ; L′ = $PPh_2N^{(-)i}Pr$, where ^{i}Pr = isopropyl), which like **2**-Fe_3 features three Fe-edge sites but like **1**-Fe has minimal affinity for exogenous ligands,[28] was included in this comparison. Under the same conditions, **2′**-Fe_3 was found to be the fastest catalyst in the series, with a $t_{1/2}$ of ca. 5 min (Figure 2). At first sight, the trend in the catalytic activities **2′**-Fe_3 > **1**-Fe > **2**-Fe_3 is surprising. To investigate the

Scheme 1. Stoichiometric Azide Activation and Nitrene Transfer to (a) an Isocyanide or (b) a Phosphine

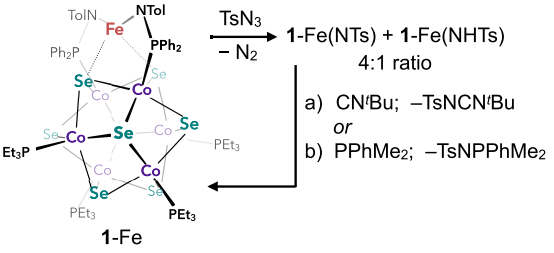

Scheme 2. Probing the Formation of 1-Fe(NHTs)

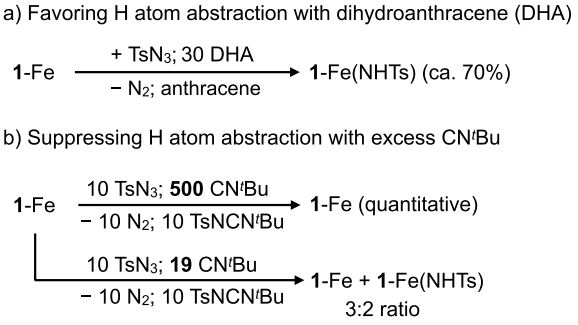

https://doi.org/10.1021/acs.inorgchem.3c01601
Inorg. Chem. 2023, 62, 8789−8793

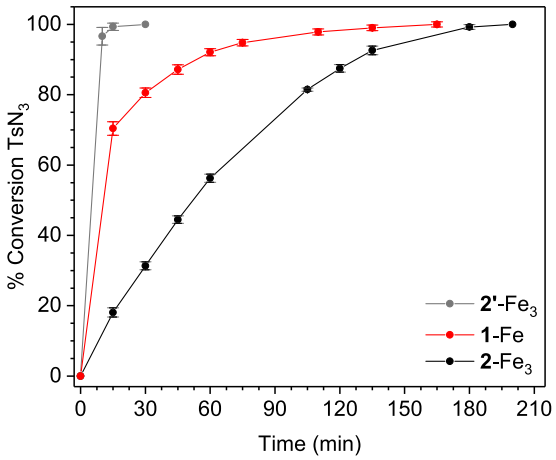

Figure 2. Comparing the catalytic activity of **1**-Fe, **2**-Fe_3, and **2′**-Fe_3 toward carbodiimide formation from TsN_3 and ^{t}BuNC at 2.5% cluster loading, 5.6 M ^{t}BuNC, in benzene-d_6 at room temperature.

origins of the differential reactivity in the series, electrochemical, structural, substrate affinity, and vibrational data are compared below, revealing that catalytic activity peaks when metal/support interactions are strongest and the affinity for isocyanide is lowest.

In part, this trend in the reactivity stems from the dual role that isocyanide plays in this transformation. While increased concentration of ^{t}BuNC prevents cluster degradation, ostensibly by accelerating nitrene transfer, it also inhibits reactivity by blocking azide coordination at Fe. This effect is qualitatively illustrated in the slower catalytic activity for **1**-Fe upon the concentration of isocyanide is increased from 0.2 to 5.6 M (Figure S14). In **2**-Fe_3 and **2′**-Fe_3, this behavior is compounded by interadsorbate effects stemming from the presence of multiple active sites.

Comparing the relative HOMO energies of the clusters, approximated from cyclic voltammetry measurements, indicates that the clusters are increasingly electron-rich in the series **2**-Fe_3 < **2′**-Fe_3 < **1**-Fe, with the 0/1+ oxidation event ranging from −0.6 to −1.0 V vs Fc/Fc^+ (Figure 3a).[15,16,28] This cathodic shift can be rationalized by the relative number of Lewis acidic edges (one in **1**-Fe vs three in **2**-Fe_3 and **2′**-Fe_3) and the donating properties of the ancillary ligands (PEt_3 in **1**-Fe vs $PPh_2N^{(-)}$Tol in **2**-Fe_3; $PPh_2N^{(-)}$ Tol in **2**-Fe_3 vs $PPh_2N^{(-)i}$Pr in **2′**-Fe_3).

Previously reported structural data[15,16,28] report that qualitatively Fe−Se bonds are strongest in **1**-Fe, where the Se sites are most electron-rich, and weakest in **2**-Fe_3, where they are most electronically depleted (Figure 1). A precise structural comparison is complicated because **2**-$Fe_3(CN^tBu)_3$, crystallized as a tris-adduct, features only one Fe−Se per edge.[15,16,28]

Finally, the strengths of the metal/substrate and metal/support interactions are inversely related, and the nature of the Fe−CN^tBu interaction is highly sensitive to distal changes in the clusters. The affinity for isocyanide at Fe, estimated using ^{1}H NMR spectroscopy, is low for the electron-rich clusters **1**-Fe and **2′**-Fe_3 (~26 and 7 M^{-1}, respectively; Figure S19) and significantly higher for the more electron-deficient **2**-Fe_3, where three binding constants could be resolved (1290, 196, and 19 M^{-1}, respectively),[15,16] ostensibly for each Fe edge. In line with the estimated isocyanide affinities, **1**-Fe and **2′**-Fe_3 crystallize free of exogeneous ligands even in the presence of a large excess of ^{t}BuNC (100 equiv), whereas **2**-Fe_3 can be isolated as the tris-adduct **2**-$Fe_3(CN^tBu)_3$. Beyond the affinity for ligands, IR spectroscopy reveals that the edge sites in **1**-Fe and **2′**-Fe_3 are sufficiently electron-rich to π-backbond and activate the isocyanide (ν_{CN} = 2088 and 2104 cm^{-1}, respectively), whereas the blue-shifted CN stretch in **2**-$Fe_3(CN^tBu)_x$ (ν_{CN} = 2168 cm^{-1}) signals that only σ-bonding is present (Figure 3b). This indicates that the strongest isocyanide activation occurs at the Fe-edge sites with the lowest affinity for this ligand.

It is attractive to propose that the increased catalytic activity of **2′**-Fe_3 versus **1**-Fe stems from a higher number of active sites (three vs one). Both clusters are more active catalysts than **2**-Fe_3, in line with their decreased affinity for isocyanide and increased electronic richness. However, in spite of the electronic and structural similarities across the series, different reaction mechanisms could be at play.[24,29−36] Furthermore, the extent Co_6Se_8 electronic participation in the **1**-Fe, **2′**-Fe_3, and **2**-Fe_3 series could vary, giving rise to different edge/core redox regimes and distinguishing the reactivity of iron nitrenoid species formed along the way.[15]

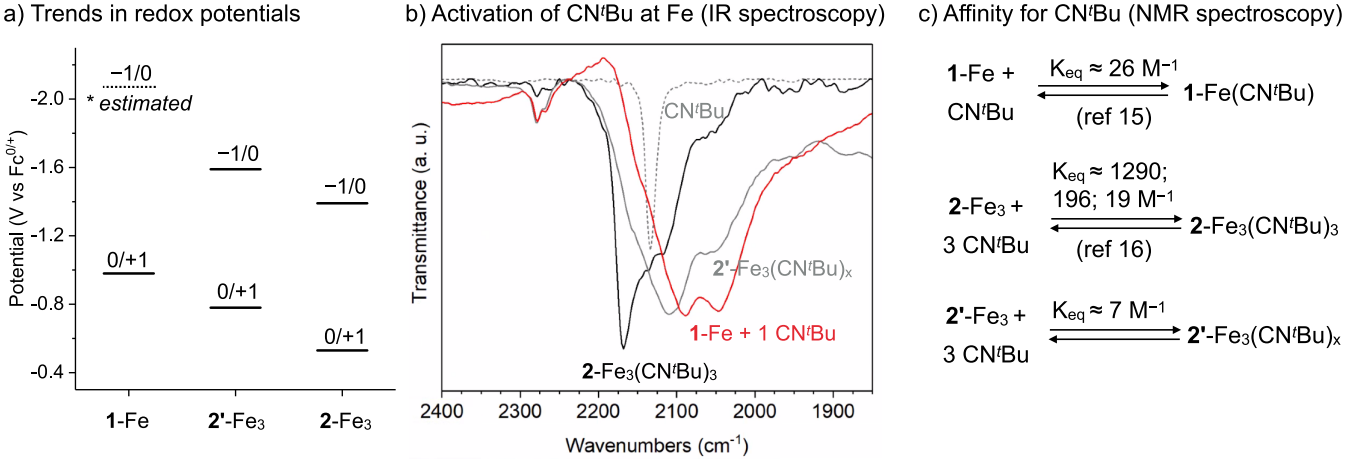

Figure 3. Comparing the electronic properties of the Fe-edge sites in **1**-Fe, **2**-Fe_3, and **2′**-Fe_3. (a) HOMO/LUMO energies estimated electrochemically. (b) Electrophilicity of the Fe-edge sites as proxied by the energy of bound isocyanide, measured via IR spectroscopy. (c) Affinity for isocyanide, measured by NMR spectroscopy.

https://doi.org/10.1021/acs.inorgchem.3c01601
Inorg. Chem. 2023, 62, 8789−8793

In conclusion, adjusting the electronic profile of the Fe-edge sites via distal changes in the cluster, such as the number of neighboring active sites or the nature of capping ligands, regulates the affinity for substrates at the Fe edge and tunes the catalytic activity. As the support cluster becomes more electronically rich, the metal/support interactions (Fe−Se bonds) are strengthened, while the metal/substrate (Fe−CN^{t}Bu) interactions become more labile. The dynamic, push−pull interactions between the substrate (^{t}BuNC), active site (Fe), and support (Co_6Se_8) foster a substrate binding behavior, wherein substrate activation occurs with its expedited release, enabling increased catalytic activity.

■ ASSOCIATED CONTENT

Supporting Information

The Supporting Information is available free of charge at https://pubs.acs.org/doi/10.1021/acs.inorgchem.3c01601.

General experimental considerations, catalytic and stoichiometric nitrene transfer studies, hydrogen-atom abstraction experiments, and binding constant analysis (PDF)

■ AUTHOR INFORMATION

Corresponding Author

Alexandra Velian − *Department of Chemistry, University of Washington, Seattle, Washington 98195, United States;* orcid.org/0000-0002-6782-7139; Email: avelian@uw.edu

Authors

Benjamin S. Mitchell − *Department of Chemistry, University of Washington, Seattle, Washington 98195, United States;* orcid.org/0000-0001-6585-2237

Andrei Chirila − *Department of Chemistry, University of Washington, Seattle, Washington 98195, United States*

Daniel Y. Zhou − *Department of Chemistry, University of Washington, Seattle, Washington 98195, United States*

Jonathan A. Kephart − *Department of Chemistry, University of Washington, Seattle, Washington 98195, United States;* orcid.org/0000-0003-4608-1160

Complete contact information is available at: https://pubs.acs.org/10.1021/acs.inorgchem.3c01601

Notes

The authors declare no competing financial interest.

■ ACKNOWLEDGMENTS

This work was supported by the National Science Foundation (NSF) through a Faculty Early Career Development Program Award (1944843) and by the Research Corporation for Science Advancement through a Cottrell Scholars Award. B.S.M. is grateful for support from the NSF Graduate Research Fellowship Program, and the University of Washington Clean Energy Institute Graduate Fellowship.

■ REFERENCES

(1) Sabatier, P. (1854−1941) A. du texte. *La Catalyse En Chimie Organique*; Paris et Liége, 1913.

(2) Trasatti, S. Work Function, Electronegativity, and Electrochemical Behaviour of Metals: III. Electrolytic Hydrogen Evolution in Acid Solutions. *J. Electroanal. Chem. Interfacial Electrochem.* **1972**, *39* (1), 163−184.

(3) Medford, A. J.; Vojvodic, A.; Hummelshøj, J. S.; Voss, J.; Abild-Pedersen, F.; Studt, F.; Bligaard, T.; Nilsson, A.; Nørskov, J. K. From the Sabatier Principle to a Predictive Theory of Transition-Metal Heterogeneous Catalysis. *J. Catal.* **2015**, *328*, 36−42.

(4) Oudar, J. *Deactivation and Poisoning of Catalysts*; CRC Press, 1985.

(5) Chikan, V.; Kelley, D. F. Size-Dependent Spectroscopy of MoS_2 Nanoclusters. *J. Phys. Chem. B* **2002**, *106* (15), 3794−3804.

(6) Tuxen, A.; Kibsgaard, J.; Gøbel, H.; Lægsgaard, E.; Topsøe, H.; Lauritsen, J. V.; Besenbacher, F. Size Threshold in the Dibenzothiophene Adsorption on MoS_2 Nanoclusters. *ACS Nano* **2010**, *4* (8), 4677−4682.

(7) Bruix, A.; Lauritsen, J. V.; Hammer, B. Effects of Particle Size and Edge Structure on the Electronic Structure, Spectroscopic Features, and Chemical Properties of Au(111)-Supported MoS_2 Nanoparticles. *Faraday Discuss.* **2016**, *188* (0), 323−343.

(8) Wu, Z.; Fang, B.; Wang, Z.; Wang, C.; Liu, Z.; Liu, F.; Wang, W.; Alfantazi, A.; Wang, D.; Wilkinson, D. P. MoS_2 Nanosheets: A Designed Structure with High Active Site Density for the Hydrogen Evolution Reaction. *ACS Catal.* **2013**, *3* (9), 2101−2107.

(9) Hakala, M.; Kronberg, R.; Laasonen, K. Hydrogen Adsorption on Doped MoS2 Nanostructures. *Sci. Rep.* **2017**, *7* (1), 15243.

(10) Pérez-Ramírez, J.; López, N. Strategies to Break Linear Scaling Relationships. *Nat. Catal.* **2019**, *2* (11), 971−976.

(11) Arnett, C. H.; Kaiser, J. T.; Agapie, T. Remote Ligand Modifications Tune Electronic Distribution and Reactivity in Site-Differentiated, High-Spin Iron Clusters: Flipping Scaling Relationships. *Inorg. Chem.* **2019**, *58* (23), 15971−15982.

(12) Hernández Sánchez, R.; Champsaur, A. M.; Choi, B.; Wang, S. G.; Bu, W.; Roy, X.; Chen, Y.-S.; Steigerwald, M. L.; Nuckolls, C.; Paley, D. W. Electron Cartography in Clusters. *Angew. Chem., Int. Ed.* **2018**, *57* (42), 13815−13820.

(13) Amtawong, J.; Nguyen, A. I.; Tilley, T. D. Mechanistic Aspects of Cobalt−Oxo Cubane Clusters in Oxidation Chemistry. *J. Am. Chem. Soc.* **2022**, *144* (4), 1475−1492.

(14) Sridharan, A.; Brown, A. C.; Suess, D. L. M. A Terminal Imido Complex of an Iron−Sulfur Cluster. *Angew. Chem., Int. Ed.* **2021**, *60* (23), 12802−12806.

(15) Mitchell, B. S.; Chirila, A.; Kephart, J. A.; Boggiano, A. C.; Krajewski, S. M.; Rogers, D.; Kaminsky, W.; Velian, A. Metal−Support Interactions in Molecular Single-Site Cluster Catalysts. *J. Am. Chem. Soc.* **2022**, *144* (40), 18459−18469.

(16) Kephart, J. A.; Mitchell, B. S.; Chirila, A.; Anderton, K. J.; Rogers, D.; Kaminsky, W.; Velian, A. Atomically Defined Nanopropeller $Fe_3Co_6Se_8(Ph_2PNTol)_6$: Functional Model for the Electronic Metal−Support Interaction Effect and High Catalytic Activity for Carbodiimide Formation. *J. Am. Chem. Soc.* **2019**, *141* (50), 19605−19610.

(17) Mitchell, B. S.; Krajewski, S. M.; Kephart, J. A.; Rogers, D.; Kaminsky, W.; Velian, A. Redox-Switchable Allosteric Effects in Molecular Clusters. *JACS Au* **2022**, *2* (1), 92−96.

(18) Kephart, J. A.; Mitchell, B. S.; Kaminsky, W.; Velian, A. Multi-Active Site Dynamics on a Molecular Cr/Co/Se Cluster Catalyst. *J. Am. Chem. Soc.* **2022**, *144* (21), 9206−9211.

(19) Mitchell, B. S.; Kaminsky, W.; Velian, A. Tuning the Electronic Structure of Atomically Precise Sn/Co/Se Nanoclusters via Redox Matching of Tin(IV) Surface Sites. *Inorg. Chem.* **2021**, *60* (9), 6135−6139.

(20) Mitchell, B.; Chirila, A.; Zhou, D.; Kephart, J.; Velian, A. Metal−Support Interactions Regulate Substrate Binding in Fe/Co/Se Cluster Catalysts. *ChemRxiv*, Nov 24, 2022. DOI: 10.26434/chemrxiv-2022-f19xz (accessed 2023-05-15).

(21) Harlan, E. W.; Holm, R. H. Molybdenum-Mediated Imido Group Transfer: Stoichiometric and Catalytic Reactions and Structures. *J. Am. Chem. Soc.* **1990**, *112* (1), 186−193.

(22) Wilding, M. J. T.; Iovan, D. A.; Betley, T. A. High-Spin Iron Imido Complexes Competent for C−H Bond Amination. *J. Am. Chem. Soc.* **2017**, *139* (34), 12043−12049.

(23) King, E. R.; Hennessy, E. T.; Betley, T. A. Catalytic C−H Bond Amination from High-Spin Iron Imido Complexes. *J. Am. Chem. Soc.* **2011**, *133* (13), 4917−4923.
(24) Spasyuk, D. M.; Carpenter, S. H.; Kefalidis, C. E.; Piers, W. E.; Neidig, M. L.; Maron, L. Facile Hydrogen Atom Transfer to Iron(III) Imido Radical Complexes Supported by a Dianionic Pentadentate Ligand. *Chem. Sci.* **2016**, *7* (9), 5939−5944.
(25) Mayer, J. M. Understanding Hydrogen Atom Transfer: From Bond Strengths to Marcus Theory. *Acc. Chem. Res.* **2011**, *44* (1), 36−46.
(26) Roberts, B. P. Polarity-Reversal Catalysis of Hydrogen-Atom Abstraction Reactions: Concepts and Applications in Organic Chemistry. *Chem. Soc. Rev.* **1999**, *28* (1), 25−35.
(27) Bietti, M.; Cucinotta, E.; DiLabio, G. A.; Lanzalunga, O.; Lapi, A.; Mazzonna, M.; Romero-Montalvo, E.; Salamone, M. Evaluation of Polar Effects in Hydrogen Atom Transfer Reactions from Activated Phenols. *J. Org. Chem.* **2019**, *84* (4), 1778−1786.
(28) Kephart, J. A.; Boggiano, A. C.; Kaminsky, W.; Velian, A. Inorganic Clusters as Metalloligands: Ligand Effects on the Synthesis and Properties of Ternary Nanopropeller Clusters. *Dalton Trans.* **2020**, *49* (45), 16464−16473.
(29) Cowley, R. E.; Golder, M. R.; Eckert, N. A.; Al-Afyouni, M. H.; Holland, P. L. Mechanism of Catalytic Nitrene Transfer Using Iron(I)−Isocyanide Complexes. *Organometallics* **2013**, *32* (19), 5289−5298.
(30) Yang, Y.; Diederich, F.; Valentine, J. S. Lewis Acidic Catalysts for Olefin Epoxidation by Iodosylbenzene. *J. Am. Chem. Soc.* **1991**, *113* (19), 7195−7205.
(31) Li, Z.; Quan, R. W.; Jacobsen, E. N. Mechanism of the (Diimine)Copper-Catalyzed Asymmetric Aziridination of Alkenes. Nitrene Transfer via Ligand-Accelerated Catalysis. *J. Am. Chem. Soc.* **1995**, *117* (21), 5889−5890.
(32) Roose, T. R.; Verdoorn, D. S.; Mampuys, P.; Ruijter, E.; Maes, B. U. W.; Orru, R. V. A. Transition Metal-Catalysed Carbene- and Nitrene Transfer to Carbon Monoxide and Isocyanides. *Chem. Soc. Rev.* **2022**, *51* (14), 5842−5877.
(33) Laskowski, C. A.; Hillhouse, G. L. Group-Transfer Reactions of Ni(II)−Ni(II) Bridging Imido Complexes. Catalytic Formation of Carbodiimides and Isocyanates via Nitrene Transfer from Organo-azides. *Organometallics* **2009**, *28* (20), 6114−6120.
(34) Yousif, M.; Tjapkes, D. J.; Lord, R. L.; Groysman, S. Catalytic Formation of Asymmetric Carbodiimides at Mononuclear Chromium(II/IV) Bis(Alkoxide) Complexes. *Organometallics* **2015**, *34* (20), 5119−5128.
(35) Beaumier, E. P.; McGreal, M. E.; Pancoast, A. R.; Wilson, R. H.; Moore, J. T.; Graziano, B. J.; Goodpaster, J. D.; Tonks, I. A. Carbodiimide Synthesis via Ti-Catalyzed Nitrene Transfer from Diazenes to Isocyanides. *ACS Catal.* **2019**, *9* (12), 11753−11762.
(36) Nguyen, A. I.; Zarkesh, R. A.; Lacy, D. C.; Thorson, M. K.; Heyduk, A. F. Catalytic Nitrene Transfer by a Zirconium(IV) Redox-Active Ligand Complex. *Chem. Sci.* **2011**, *2* (1), 166−169.

https://doi.org/10.1021/acs.inorgchem.3c01601
Inorg. Chem. 2023, 62, 8789−8793